

# A collisional–radiative model applicable to argon discharges over a wide range of conditions.

## I: Formulation and basic data

J Vlček

Department of Physics, Institute of Mechanical and Electrical Engineering,  
306 14 Pízeň, Nejedlého sady 14, Czechoslovakia

Received 12 July 1988, in final form 28 November 1988

**Abstract.** A collisional–radiative model with an extended region of applicability is developed for an argon atom plasma. Atom–atom inelastic collisions and diffusion losses of the metastable states along with the electron–atom inelastic collisions and radiative processes are considered in this model, taking into account 65 effective levels. Among the analytical expressions used for the corresponding cross sections, special attention is paid to those determining the set of cross sections for excitation by electrons from the ground state, owing to the possibility of utilising the formulae recommended in kinetic modelling studies of discharges in argon or in mixtures including argon atoms. The numerical method developed makes it possible to investigate the mechanisms by which the excited levels are populated in a non-equilibrium argon plasma characterised (even in the case of a non-Maxwellian electron distribution) by a set of parameters, such as the electron kinetic temperature  $T_e$ , the atom temperature  $T_a$ , the ion temperature  $T_i$ , the electron number density  $n_e$ , the ground state atom population  $n_1$ , the discharge tube (or the plasma column) radius  $R$  and the optical escape factors  $\Lambda_{m1}$  and  $\Lambda_{m2}$ , which are dependent only on the quantities  $T_a$ ,  $n_1$  and  $R$  in many cases of practical interest.

### 1. Introduction

One of the simplifying assumptions made in basic equations describing the extensive collisional–radiative (CR) models (see e.g. Bates *et al* 1962, Drawin and Emard 1977, Fujimoto 1979, Biberman *et al* 1982, van der Sijde *et al* 1984) is the use of the Maxwellian electron energy distribution function (EEDF). However, it has been shown by many authors that this assumption is unjustified for a wide range of physically interesting conditions in various gases.

In our recent papers (Vlček and Pelikán 1985, 1986), we presented a numerical method which enabled us to extend the applicability of the existing extensive CR models for the argon atom plasma with the Maxwellian distribution function (Giannaris and Incropera 1973, Katsonis 1976, Gomés 1983, van der Sijde *et al* 1984, Hasegawa and Haraguchi 1985) to the region in which the actual EEDF differs appreciably from the Maxwellian form.

A substantial feature of this method is a numerical solution of the Boltzmann equation (Vlček and Pelikán 1985) for the EEDF in a non-equilibrium argon plasma

characterised by a set of parameters, such as the electron kinetic temperature  $T_e$ , the atom temperature  $T_a$ , the ion temperature  $T_i$ , the electron number density  $n_e$  and the ground state atom population  $n_1$ , which are in accordance with the usual input parameters of the basic equations for the CR models.

Here, our objective is to present an extensive CR model which may be applied to argon discharges in a wide range of practically interesting conditions.

We have used the slightly corrected argon atom model of Drawin and Katsonis (1976) which includes 65 discrete effective levels and reflects the actual atomic structure.

In addition to the possibility of using a realistic EEDF, two further modifications have been carried out in the usual formulation of the basic equations for the CR models: the atom–atom inelastic collisions and the diffusion losses of the two metastable states are considered.

In choosing the analytical expressions for the cross sections, we have taken into account the most recent experimental and theoretical results available for argon in the literature. In particular, we have used extensively

the measurements of Chutjian and Cartwright (1981) and the computations of Kimura *et al* (1985).

The local effect of radiation trapping is described by introducing the optical escape factors which represent further input parameters in our model calculations. However, in many cases of practical interest only the reabsorption of resonance radiation is important and the corresponding escape factors are dependent only on the quantities  $T_a$ ,  $n_1$  and  $R$  mentioned above (Walsh 1959, Mills and Hieftje 1984).

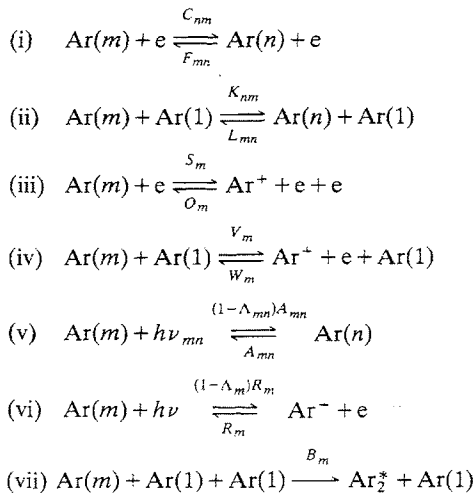
The numerical method developed makes it possible to investigate the mechanisms by which the excited levels in various practically interesting argon discharges are populated, such as low-pressure glow discharges, hollow cathode discharges, atmospheric or sub-atmospheric arcs and ICP discharges.

## 2. Formal solution of the problem

We will confine ourselves to a quasi-neutral argon plasma composed of atoms Ar, free electrons e and only singly ionised ions  $\text{Ar}^+$  in the ground state with the number density  $n_+ = n_e$ .

Our computations are based on the argon atom model of Drawin and Katsonis (1976), in which we have separated the resonance and metastable states originally grouped together in the two lowest excited effective levels. We consider 64 excited effective levels divided into two subsystems, corresponding to either of the two core quantum numbers  $j_c = \frac{1}{2}$  ('primed system') and  $j_c = \frac{3}{2}$  ('unprimed system'). Then the idealised model has two different ionisation limits referring to the core configurations  $^2\text{P}_{1/2}$  and  $^2\text{P}_{3/2}$ , respectively, as the actual argon atom. Basic data characterising the 65 effective levels considered and numbered according to their ionisation energies are given in table 1.

The following collisional and radiative processes, together with the diffusion losses of the metastables, are considered in our extended version of the CR model:



where  $m = 2$  and 4.

(viii) diffusion of the metastables  $4s[3/2]_2$  and  $4s'[1/2]_0$  (for which  $n=2$  and 4 in table 1, respectively) to the wall.

Here,  $C_{nm}$  and  $K_{nm}$  are the rate coefficients for collisional excitation by electrons and by ground state atoms respectively.  $F_{mn}$  and  $L_{mn}$  are respectively the rate coefficients for the inverse processes (collisional de-excitations).  $S_m$  and  $V_m$  are the corresponding collisional ionisation rate coefficients while  $O_m$  and  $W_m$  are the rate coefficients for the inverse three-body recombinations and  $R_m$  is the radiative recombination rate coefficient.  $A_{mn}$  is the transition probability,  $\Lambda_{mn}$  and  $\Lambda_m$  are the optical escape factors for bound-bound and bound-free transitions, respectively.  $B_m$  is the rate constant for the three-body collisions of metastable states with the ground state atoms.

Under conditions allowing the use of the quasi-stationary state model (discussed in greater detail by Bates *et al* 1962, Cacciatore *et al* 1976, Biberman *et al* 1982) and calculation of the rate of loss of the metastables by diffusion to the wall, assuming that their radial distribution corresponds to the fundamental diffusion mode for the discharge tube (see e.g. Delcroix *et al* 1976, Ferreira *et al* 1985), we obtain a set of coupled linear equations

$$\sum_{n=2}^{65} a_{mn} n_n = -\delta_m - a_{m1} n_1 \quad (1)$$

where  $m = 2, \dots, 65$ , from which the unknown excited level populations  $n_n$  may be calculated provided that the coefficients  $a_{mn}$  and  $\delta_m$  are known and the ground state atom population  $n_1$  has been determined experimentally.

The coefficients  $a_{mn}$  and  $\delta_m$  are related to the above-mentioned processes (i)–(viii) by the expressions

$$a_{mn} = n_e C_{mn} + n_1 K_{mn} \quad m > n \quad (2)$$

$$a_{mn} = n_e F_{mn} + n_1 L_{mn} + \Lambda_{mn} A_{mn} \quad m < n \quad (3)$$

$$a_{nn} = -(n_e S_n + n_1 V_n + \sum_{\substack{m=1 \\ m \neq n}}^{65} a_{mn} + D_n/\Lambda^2 + n_1^2 B_n) \quad m = n \quad (4)$$

$$\delta_m = n_e n_+ (n_e O_m + n_1 W_m + \Lambda_m R_m). \quad (5)$$

Let us recall that in our model the diffusion coefficient  $D_n$  and the three-body rate constant  $B_n$ , appearing in (4), are non-zero only when  $n = 2$  and  $n = 4$ .

Assuming diffusion in the fundamental mode is dominant in a discharge tube of length  $L$ ,  $L \gg R$ , where  $R$  is the radius of the tube, and the temperature dependence of the diffusion coefficients  $D_n$  in argon is the same as in neon (Phelps 1959), the diffusion term in (4) can be rewritten in the form  $d_n T_a^{0.75}/n_1 R^2$ , where  $d_n$  is a constant given by the experimental data for  $D_n n_1$  (Tachibana 1986). The values of  $B_n$  are also taken from Tachibana (1986).

The expressions for the rate coefficients referring to the inelastic collisions under consideration are obtained

**Table 1.** Data characterising the excited levels considered in the model and the transition-dependent parameters (see main text) relating to the cross sections for excitation by electrons from the ground state. A, optically allowed; P, parity-forbidden; S, spin-forbidden transitions.

Level number $n$	Designation $n_{pqnl} [K]_J$	Excitation energy $\varepsilon_{1n}$ (eV)	Statistical weight $g_n$	Nature of transition	Transition-dependent parameters $\alpha_{1n}^A = \alpha_{1n}^A f_{1n}$ and $\beta_{1n}$ , or $\alpha_{1n}^P$ , or $\alpha_{1n}^S$
1	3p <sup>6</sup>	0.000	1	—	—
2	4s[3/2] <sub>2</sub>	11.548	5	S	$6.70 \times 10^{-2}$
3	4s[3/2] <sub>1</sub>	11.624	3	A	$1.92 \times 10^{-2}$ , 4.00
4	4s'[1/2] <sub>0</sub>	11.723	1	S	$9.50 \times 10^{-3}$
5	4s'[1/2] <sub>1</sub>	11.828	3	A	$4.62 \times 10^{-2}$ , 4.00
6	4p[1/2] <sub>1</sub>	12.907	3	P	$3.50 \times 10^{-2}$
7	4p[3/2] <sub>1,2</sub> , [5/2] <sub>2,3</sub>	13.116	20	P	$1.15 \times 10^{-1}$
8	4p'[3/2] <sub>1,2</sub>	13.295	8	P	$3.50 \times 10^{-2}$
9	4p'[1/2] <sub>1</sub>	13.328	3	P	$7.00 \times 10^{-3}$
10	4p[1/2] <sub>0</sub>	13.273	1	P	$7.00 \times 10^{-3}$
11	4p'[1/2] <sub>0</sub>	13.480	1	P	$3.50 \times 10^{-2}$
12	3d[1/2] <sub>0,1</sub> , [3/2] <sub>2</sub>	13.884	9	S	$1.50 \times 10^{-1}$
13	3d[7/2] <sub>3,4</sub>	13.994	16	S	$9.00 \times 10^{-2}$
14	3d'[3/2] <sub>2</sub> , [5/2] <sub>2,3</sub>	14.229	17	P	$4.20 \times 10^{-2}$
15	5s'	14.252	4	A	$3.71 \times 10^{-3}$ , 4.00
16	3d[3/2] <sub>1</sub> , [5/2] <sub>2,3</sub> + 5s	14.090	23	A	$3.33 \times 10^{-2}$ , 4.00
17	3d'[3/2] <sub>1</sub>	14.304	3	A	$1.79 \times 10^{-2}$ , 2.00
18	5p	14.509	24	P	$7.00 \times 10^{-2}$
19	5p'	14.690	12	P	$5.00 \times 10^{-2}$
20	4d + 6s	14.792	48	A	$5.15 \times 10^{-2}$ , 1.00
21	4d' + 6s'	14.976	24	A	$3.06 \times 10^{-2}$ , 1.00
22	4f'	15.083	28	—	—
23	4f	14.906	56	—	—
24	6p'	15.205	12	—	—
25	6p	15.028	24	—	—
26	5d' + 7s'	15.324	24	A	$6.50 \times 10^{-4}$ , 1.00
27	5d + 7s	15.153	48	A	$3.69 \times 10^{-2}$ , 1.00
28	5f', g'	15.393	64	—	—
29	5f, g	15.215	128	—	—
30	7p'	15.461	12	—	—
31	7p	15.282	24	—	—
32	6d' + 8s'	15.520	24	—	—
33	6d + 8s	15.347	48	A	$2.40 \times 10^{-2}$ , 1.00
34	6f', g', h'	15.560	108	—	—
35	6f, g, h	15.382	216	—	—
36	8p'	15.600	12	—	—
37	8p	15.423	24	—	—
38	7d' + 9s'	15.636	24	—	—
39	7d + 9s	15.460	48	—	—
40	7f', g', h', i'	15.659	160	—	—
41	7f, g, h, i	15.482	320	—	—
42	8d', f', ...	15.725	240	—	—
43	8d, f, ...	15.548	480	—	—
44	9p', d', f', ...	15.769	320	—	—
45	9p, d, f, ...	15.592	640	—	—
46		15.801	400	—	—
47	$n_{pqnl} = 10$	15.624	800	—	—
48		15.825	484	—	—
49	$n_{pqnl} = 11$	15.648	968	—	—
50		15.843	576	—	—
51	$n_{pqnl} = 12$	15.666	1152	—	—
52		15.857	676	—	—
53	$n_{pqnl} = 13$	15.680	1352	—	—
54		15.868	784	—	—
55	$n_{pqnl} = 14$	15.691	1568	—	—
56		15.877	900	—	—
57	$n_{pqnl} = 15$	15.700	1800	—	—
58		15.884	1024	—	—
59	$n_{pqnl} = 16$	15.707	2048	—	—
60		15.890	1156	—	—
61	$n_{pqnl} = 17$	15.713	2312	—	—
62		15.895	1296	—	—
63	$n_{pqnl} = 18$	15.718	2592	—	—
64		15.899	1444	—	—
65	$n_{pqnl} = 19$	15.722	2888	—	—

from general formulae (see e.g. Mitchner and Kruger 1973) on the basis of the reasonable assumption that the distribution function for the heavy particles is of Maxwellian form in all cases, whereas the distribution of electrons may differ from the Maxwellian function.

The only component of the EEDF to appear in the rate coefficients for the electron-atom collisions in (2)–(5) is the isotropic function  $f(u)$ , where the dimensionless energy  $u = \varepsilon/kT_e$  ( $\varepsilon$  being the electron energy and  $k$  the Boltzmann constant) is introduced.

The following integral formulae have been used for these rate coefficients (Vlček and Pelikán 1986):

$$C_{mn} = 8\pi \left(\frac{kT_e}{m_e}\right)^2 \int_{u_{mn}}^{\infty} f(u) \sigma_{nm}(u) u \, du \quad (6)$$

$$S_n = 8\pi \left(\frac{kT_e}{m_e}\right)^2 \int_{u_n}^{\infty} f(u) \sigma_n(u) u \, du \quad (7)$$

$$F_{mn} = 8\pi \left(\frac{kT_e}{m_e}\right)^2 \frac{g_m}{g_n} \int_{u_{mn}}^{\infty} f(u - u_{mn}) \sigma_{mn}(u) u \, du \quad (8)$$

$$R_m = \frac{8\pi}{c^2} \left(\frac{h}{m_e}\right)^3 \frac{g_m}{2g_+} \int_{\varepsilon_m/h}^{\infty} f(h\nu - \varepsilon_m) \sigma_m^p(\nu) \nu^2 \, d\nu \quad (9)$$

$$O_m = 8\pi \left(\frac{kT_e}{m_e}\right)^2 \frac{g_m}{2g_-} \left(\frac{h^2}{2\pi m_e kT_e}\right)^{3/2} \times \int_{u_m}^{\infty} f(u - u_m) \sigma_m(u) u \, du \quad (10)$$

Here,  $m_e$  is the electron mass,  $c$  is the velocity of light in a vacuum,  $g_-$  is the statistical weight of the ground state of the ions,  $\sigma_{nm}(u)$  and  $\sigma_{mn}(u)$  are the cross sections referring to collisional excitations by electrons from the  $n$ th excited level to the  $m$ th level and from the  $m$ th excited level to the  $n$ th level, respectively, whilst  $\sigma_m(u)$  and  $\sigma_m^p(\nu)$  are the cross sections for collisional ionisation by electrons and for photoionisation of the  $m$ th level, respectively.

Under conditions when the distribution function is non-Maxwellian, the Boltzmann equation for  $f(u)$  is solved numerically in the form (Vlček and Pelikán 1985)

$$\frac{d}{du} \left( H(u) \frac{df(u)}{du} + G(u)f(u) \right) = n_1 u M(u) f(u) \quad (11)$$

where

$$M(u) = 0 \quad u \leq u_{12}$$

$$M(u) = \sigma_{\text{exc}}(u) + \sigma_1(u) \quad u > u_{12}.$$

The formulae for the total excitation cross section  $\sigma_{\text{exc}}(u)$  and the ionisation cross section  $\sigma_1(u)$  will be characterised later.

In (11) the terms  $H(u)$  and  $G(u)$  describe the influence of the electron energy gain and loss processes, respectively, on the EEDF.  $H(u)$  includes the expressions corresponding to the Coulomb electron-electron and electron-ion interactions, the effect of the axial electric field and the thermal motion of gas atoms.  $G(u)$  is given by the sum of the terms related to the Coulomb

electron-electron and electron-ion interactions and to the elastic electron-atom collisions. The EEDF is normalised, so that

$$2\pi \left(\frac{2kT_e}{m_e}\right)^{3/2} \int_0^{\infty} u^{1/2} f(u) \, du = 1.$$

The rate coefficients for the atom-atom collisions (ii) and (iv) appearing in equations (2)–(5) are given by the following expressions (Bacri and Gomés 1978, Biberman *et al* 1982, Collins 1967):

$$K_{mn} = 2 \left(\frac{2kT_a}{\pi m_{12}}\right)^{1/2} b_{nm}(\varepsilon_{mn} + 2kT_a) \exp\left(-\frac{\varepsilon_{mn}}{kT_a}\right) \quad (12)$$

$$V_n = 2 \left(\frac{2kT_a}{\pi m_{12}}\right)^{1/2} b_n(\varepsilon_n + 2kT_a) \exp\left(-\frac{\varepsilon_n}{kT_a}\right) \quad (13)$$

$$L_{mn} = K_{nm} (g_m/g_n) \exp(\varepsilon_{mn}/kT_a) \quad (14)$$

$$W_m = V_m \frac{g_m}{2g_+} \left(\frac{h^2}{2\pi m_e kT_e}\right)^{3/2} \exp\left(\frac{\varepsilon_m}{kT_a}\right) \quad (15)$$

where  $m_{12}$  is the reduced mass of two interacting atoms.

In (12) and (13) it is assumed that the cross sections for the atom-atom excitation (ii) and the atom-atom ionisation (iv),  $Q_{mn}$  and  $Q_n$ , respectively, are linear functions of energy above the threshold, so that

$$Q_{mn} = b_{mn}(E - \varepsilon_{mn}) \quad (16)$$

and

$$Q_n = b_n(E - \varepsilon_n) \quad (17)$$

where  $E$  is the relative energy of the colliding atoms.

As has been mentioned above, the local effect of radiative absorption is described by the optical escape factors  $\Lambda_{mn}$  and  $\Lambda_m$ . This method, usually used in extensive CR models (see e.g. Bates *et al* 1962, Drawin and Emard 1977, Biberman *et al* 1982, van der Sijde *et al* 1984), cannot be considered exact but it should represent a reasonable approach which reflects real situations well.

In many cases of practical interest only the trapping of the resonance radiation is important because of the relatively large corresponding transition probabilities and high population in the ground state atom.

In our model calculations, the escape factors  $\Lambda_{1n}$  for the resonance lines are determined using the formula derived by Walsh (1959) for the imprisonment lifetime when Doppler and collision broadening of the resonance line are present simultaneously. In a cylindrical tube of radius  $R$ , where axial excitation is dominant, the following expression (Mills and Hieftje 1984) holds:

$$\Lambda_{1n} = g_0 T(R) \quad (18)$$

where  $g_0 = 1.9$  for a Doppler-broadened profile and  $g_0 = 1.3$  for one dominated by pressure broadening; the

transmission coefficient  $T(R)$  is given by

$$T(R) = T_D \exp(-\pi T_{CD}^2/4T_C^2) \\ + T_C \operatorname{erf}(\pi^{1/2} T_{CD}/2T_C).$$

Here,  $T_D$  and  $T_C$  are the transmission coefficients for pure Doppler and pressure broadening, respectively, and  $T_{CD}$  is the coefficient for pressure-broadened emission and Doppler-broadened absorption profiles defined by expressions

$$T_D = \{k_0 R [\pi \ln(k_0 R)]^{1/2}\}^{-1} \\ T_C = (a/\pi^{1/2} k_0 R)^{1/2} \\ T_{CD} = 2a/\pi [\ln(k_0 R)]^{1/2}$$

where  $k_0 R$  is the optical depth pertaining to the line centre and  $a$  is the damping coefficient (Mills and Hieftje 1984). In our case, the error function  $\operatorname{erf}(x)$  (see e.g. Abramowitz and Stegun 1964) is evaluated with the help of the realistic approximation inferred by Hastings (1955).

Note that the formulae for  $K_{mn}$  and  $V_n$  must be multiplied by the factor  $\frac{1}{2}$  when  $n = 1$  in (2) and (4), respectively (see e.g. Mitchner and Kruger 1973). Furthermore, according to Katsonis (1976), the statistical weight  $g_m$  is equal to  $\frac{1}{2}$  or  $\frac{3}{2}$  for  $m = 1$  in (8) and (14) when  $n$  is the number of the level with  $j_c$  equal to  $\frac{1}{2}$  or  $\frac{3}{2}$ , respectively. Similarly,  $g_+$  is equal to 2 or 4 for  $m \geq 2$  in (9), (10) and (15) and  $n_+$  is equal to  $\frac{1}{2}n_c$  or  $\frac{3}{2}n_c$  for  $m \geq 2$  in (5) when  $m$  denotes a level corresponding to  $j_c = \frac{1}{2}$  or  $j_c = \frac{3}{2}$ , respectively.

Owing to the possibility of investigating the effect of the upward ionisation flow of electrons from the ground state atom and their downward recombination flow from a continuum when excited levels are populated (Fujimoto 1979), the system (1) is solved, in spite of the fact that  $n_1$  is not an independent parameter in our case, in the standard form

$$n_n = n_n^{(0)} + G_n^{(1)} n_1 \quad n = 2, \dots, 65 \quad (19)$$

where the population coefficients  $n_n^{(0)}$  and  $G_n^{(1)}$  are obtained from equations (1) when we insert  $n_1 = 0$  or  $n_1 = 1$  and  $\delta_m = 0$ , respectively, in their right-hand sides.

The numerical method developed allows us to calculate the population coefficients  $n_n^{(0)}$  and  $G_n^{(1)}$  as functions of the following input parameters:  $T_e$ ,  $T_a$ ,  $T_i$ ,  $n_e$ ,  $n_1$ ,  $R$  and of the escape factors  $\Lambda_{mn}$  and  $\Lambda_m$ , which are given by  $T_a$ ,  $n_1$  and  $R$  only in a wide range of practically interesting conditions. It is based on the extension of the method described in our previous papers (Vlček and Pelikán 1985, 1986). Its accuracy and reliability have been proved in many numerical tests.

### 3. Cross sections and transition probabilities

#### 3.1. Cross sections for electron-atom inelastic collisions

In the argon atom model used (see table 1) almost all the effective excited levels consist of several actual

energy states. Therefore the effective cross sections for excitation by electrons, occurring in (6) and (8), can generally be written in the form

$$\sigma_{mn} = \sigma_{mn}^A + \sigma_{mn}^F \quad (20)$$

where  $\sigma_{mn}^A$  and  $\sigma_{mn}^F$  are the cross sections for optically allowed transitions, for which  $\Delta l = \pm 1$ ,  $\Delta J = \pm 1$  with the restriction  $J = 0 \rightarrow J = 0$ , and forbidden transitions, respectively.

A lack of experimental values and a need to employ a coherent data system require the use of some analytical expressions proposed for the cross sections referring to the electron-atom inelastic collisions considered (see e.g. Drawin 1967, Biberman *et al* 1982, van der Sijde *et al* 1984, Kimura *et al* 1985). Of these, we have preferred the semi-empirical formulae of Drawin (1967), because when their scaling parameters are well chosen, they agree well with the experimental data available for argon in literature. Moreover, Drawin's parameters for numerous optically allowed and parity-forbidden transitions between excited levels in argon have been calculated recently (Kimura *et al* 1985).

We have utilised the following formulae for  $\sigma_{mn}^A$  and  $\sigma_{mn}^F$  in (20):

$$\sigma_{mn}^A = 4\pi a_0^2 \left( \frac{\varepsilon_1^H}{\varepsilon_{mn}} \right)^2 f_{mn} \alpha_{mn}^A U_{mn}^{-2} (U_{mn} - 1) \\ \times \ln(1.25 \beta_{mn} U_{mn}) \quad (21)$$

and

$$\sigma_{mn}^F \equiv \sigma_{mn}^P = 4\pi a_0^2 \alpha_{mn}^P U_{mn}^{-1} (1 - U_{mn}^{-1}) \quad (22)$$

or

$$\sigma_{mn}^F \equiv \sigma_{mn}^S = 4\pi a_0^2 \alpha_{mn}^S U_{mn}^{-3} (1 - U_{mn}^{-2}). \quad (23)$$

Here,  $U_{mn} = \varepsilon/\varepsilon_{mn}$ ,  $\varepsilon_1^H$  is the ionisation energy for atomic hydrogen in the ground state,  $a_0$  the first Bohr radius of the H atom,  $f_{mn}$  is the oscillator strength for electric dipole transition,  $\alpha_{mn}$  and  $\beta_{mn}$  are transition-dependent parameters, P and S symbolise parity- and spin-forbidden transitions, respectively. As will be shown later, only transitions between the first four excited levels are not described by Drawin's formulae.

The scaling parameters relating to the cross sections recommended by us for the excitation by electrons from the ground state are given in table 1. We have taken into account all transitions studied experimentally by Chutjian and Cartwright (1981) and also those found to be important by Peterson and Allen (1972), who analysed the electron impact energy-loss spectra obtained for argon.

As can be seen in table 1, only one term is used in (20) for all effective levels regardless of the fact that the effective levels denoted by  $n = 12, 15, 16, 20, 21, 26, 27$  and 33 include both the actual states related to the ground state by allowed transitions and those related by forbidden transitions.

The evaluation of the cross sections for the excited states  $3d[1/2]_1$ ,  $5s'[1/2]_1$ ,  $3d[3/2]_1$  and  $5s[3/2]_1$  by means of the formulae derived by Peterson and Allen (1972)



# Explore Litigation Insights

Docket Alarm provides insights to develop a more informed litigation strategy and the peace of mind of knowing you're on top of things.

## Real-Time Litigation Alerts



Keep your litigation team up-to-date with **real-time alerts** and advanced team management tools built for the enterprise, all while greatly reducing PACER spend.

Our comprehensive service means we can handle Federal, State, and Administrative courts across the country.

## Advanced Docket Research



With over 230 million records, Docket Alarm's cloud-native docket research platform finds what other services can't. Coverage includes Federal, State, plus PTAB, TTAB, ITC and NLRB decisions, all in one place.

Identify arguments that have been successful in the past with full text, pinpoint searching. Link to case law cited within any court document via Fastcase.

## Analytics At Your Fingertips



Learn what happened the last time a particular judge, opposing counsel or company faced cases similar to yours.

Advanced out-of-the-box PTAB and TTAB analytics are always at your fingertips.

## API

Docket Alarm offers a powerful API (application programming interface) to developers that want to integrate case filings into their apps.

## LAW FIRMS

Build custom dashboards for your attorneys and clients with live data direct from the court.

Automate many repetitive legal tasks like conflict checks, document management, and marketing.

## FINANCIAL INSTITUTIONS

Litigation and bankruptcy checks for companies and debtors.

## E-DISCOVERY AND LEGAL VENDORS

Sync your system to PACER to automate legal marketing.